metals

MDPI

Article

A Study of Crevice Corrosion Susceptibility of Zn-Al Alloys in a High-pH Environment

Mohammed I. Abdulsalam

Department of Chemical and Materials Engineering, Faculty of Engineering, King Abdulaziz University, Jeddah 21589, Saudi Arabia; mabdulsalam@kau.edu.sa

Abstract: This paper aims to clarify the effect of polymer coating damage of dual polymer–zinc coating used to protect rebar reinforcement from corrosion. The coating damage can result in crevices between the two materials. At these crevices, corrosion–passivation plays an important role in the integrity of the intended coating and the protectiveness of the steel base metal. An experimental design was developed to replicate a crevice of Zn-2%Al alloy. This alloy is commonly used for the dual coating protection of rebars. Experiments in this investigation were performed to test several crevice sizes and conditions to assess the state of crevice corrosion. Prepared electrodes were submerged in a 1 M NaOH solution and connected to a data logger to monitor the potential. A special reference electrode was prepared using activated titanium, against which the potential was measured. Additionally, electrochemical impedance spectroscopy (EIS) and potentiodynamic polarization were carried out to assess the corrosion rate of the different specimens. The results suggest that, in the absence of a crevice, corrosion occurred on bare specimens. However, whenever a crevice was present, a shift in potential and corrosion rate values indicated that the specimen shifted from an active corrosion regime to a passive one. This shift (gain) in potential was measured as approximately 0.9 V, resulting in a shift in the electrode potential to −0.6 V (SCE). The analysis showed that the solution inside the crevice shifted toward lower pH values, with pH = 12 suggested as the level that supports more passivity inside the crevice according to the Pourbaix diagram.

Keywords: crevice corrosion; passivation; Zn-Al alloy; EIS; rebar coating

Citation: Abdulsalam, M.I. A Study of Crevice Corrosion Susceptibility of Zn-Al Alloys in a High-pH Environment. *Metals* **2023**, *13*, 1698. https://doi.org/10.3390/met13101698

Academic Editor: Davood Nakhaie

Received: 10 September 2023
Revised: 26 September 2023
Accepted: 4 October 2023
Published: 6 October 2023

1. Introduction

Crevice corrosion is one of the many types of mechanisms through which metallic materials may deteriorate by means of local interaction between the metal and the surrounding occluded environment [1–5]. This particular type of corrosion attack occurs mainly in confined places where the electrolyte is stagnant. The mechanism through which corrosion occurs involves two possibilities: One is mainly based on the interactions between the electrode and the electrolyte that leads to a local aggressive chemistry change, causing the dissolution of the metal [3]. The other one, (the *IR* drop mechanism) has been proposed recently and is based on an ohmic potential drop, due to solution resistance that shifts the local potential inside the crevice to active potentials, thereby leading to the local dissolution of the metal [1,2,4,5]. This mechanism can successfully explain crevice corrosion under the convective mixing of crevice solution with bulk. Also, the crevice geometry has been found to play a contrasting role depending on the involved metal–electrolyte system [2,6]. Figure 1 shows a schematic illustration of these two mechanisms. Among the materials that are susceptible to this type of corrosion are the promoters of a passive layer such as stainless steel or aluminum, where a sudden decrease in the local pH can occur in the cavity of the crevice, which destroys the passive film and eventually leads to failure [3].

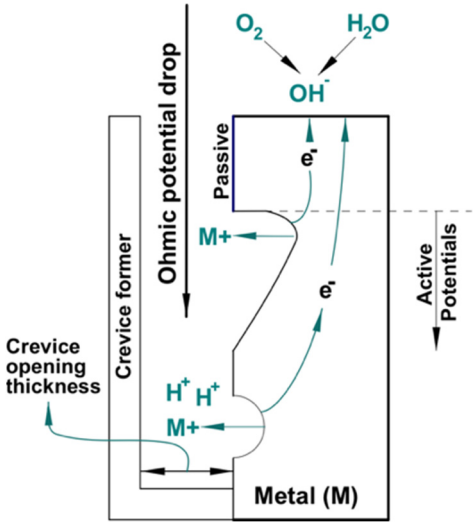

Figure 1. Crevice corrosion mechanism.

Zn coatings are used for the protection of steel rebars in concrete. However, pure zinc in certain environments is susceptible to localized intergranular corrosion [7]. Better protection is achieved when zinc is alloyed with Al [8–11]. Additionally, Al has been found to enhance ductility [12]. However, Al concentrations higher than 10% are not recommended [13]. Zn-Al alloys are widely used in industry for several applications, from anodizing pipes to galvanizing tanks, to extending the service life of the base material. Under normal conditions, aluminum forms a very thin and microscopic passive layer that can withstand most environments, while zinc between pH 8 and 13 forms corrosion products that can slow corrosion significantly [14]. However, whenever pH increases to higher values, an active corrosion regime begins due to the disruptions induced on the passive film [8,15]. Also, galvanized steel becomes less effective in chloride and sulfate solutions [16].

Better performance is achieved when galvanization is coupled with coatings. The Zn-Al alloy is also used effectively as a sacrificial anode of dual polymer–zinc coating of rebar reinforcement to further improve the corrosion protection of the conventional epoxy-coated rebar [17]. A polymer coating is intended to act as a physical barrier from aggressive chemical species on the steel surface. For example, aggressive ions like chloride ions can obstruct the protection of zinc coating, leading to failures [18]. However, polymer coatings can be subjected to damage, disbonding, and deterioration during the application of reinforced concrete. Evidently, the damage can create local occluded regions of crevice on the top of the Zn-Al coating. Further, in seawater under cathodic protection, and in the absence of galvanization, the disbonded coating crevice enhances the stress corrosion cracking of subsea pipelines [19]. These damaged areas (crevices) are of potential interest to concrete industries and therefore mandate further investigation. Thus, the current investigation aims to address this phenomenon by studying the extent of the corrosion process in specimens with active regimes and possibly those that may passivate. In order to achieve this goal, a series of experiments were carried out with specimens of varying crevice sizes, exposed to a 1 M NaOH solution for a period of 7 days. Potential transient measurements of specimens were carried out using a data logger and a solid-state activated titanium reference electrode calibrated frequently against a regular SCE electrode. The corrosion rates of the specimens were monitored by means of electrochemical impedance spectroscopy (EIS) with a frequency sweep from 10 mHz to 100 kHz. If the spectra did not show sufficient resolution for accurate corrosion rate determination, the test was conducted at a frequency of 1 mHz. Corrosion rates were then estimated using the Stern–Geary equation.

2. Experimental Procedures

2.1. Manufacturing of Specimens

Specimens for crevice corrosion testing were prepared from a Zn-2%Al alloy spool manufactured by Gerdau Knoxville ZBAR. It consists of 98 wt% Zn and 2 wt% Al. The detailed composition, as regulated by the ASTM standard specification B 833-06, is given in Table 1 [20]. The wire, approximately 1.6 mm (1/16 inches) in diameter, and segments approximately 101.6 mm (4 inches) long, were cut from the spool. Using 500-grit sandpaper, the sharp edges of the cut specimens were smoothed down until dull. By means of a 1200-grit sandpaper, the external oxide layer was removed from the surface of the specimens. Afterward, they were soaked in an acetone bath to remove any grease or oil from the surface. The crevice was created by coating the surface of the specimens with a lacquer and then inserting the specimen in a 1.52 mm diameter silicone (peroxide-cured) tube. There were two distinct regions in the specimen (Figure 2): the crevice itself (labeled *Y*) and the region leading up to the crevice (labeled X). X and Y dimensions varied among three different sizes: 7 mm, 15 mm, and 30 mm. Duplicates of each specimen were evaluated in a 1 M NaOH solution. Moreover, two control specimens were also exposed to the solution, one with nothing but a small region covered with lacquer to prevent the corrosion of the region in the solution–air interface, and the other, a completely coated control specimen.

Table 1. Chemical composition (wt.%) of zinc alloy wire 98Zn/2Al (UNS Z30402) used in this work.

Element	wt.%
Al	1.5–2.5
Cd	0.005
Cu	0.005
Fe	0.02
Pb	0.005
Sn	0.003
Sb	0.10
Ag	0.015
Bi	0.02
As	0.002
Ni	0.005
Mg	0.02
Zn	remainder

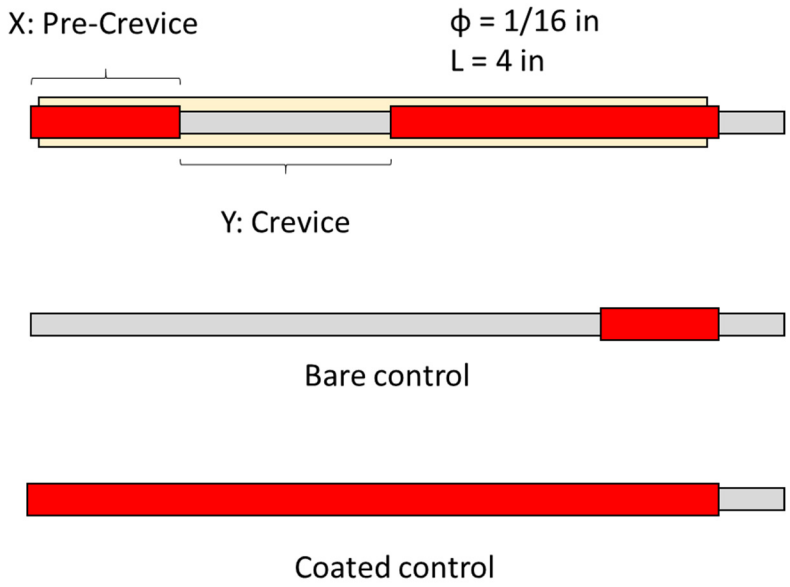

Figure 2. Description of the specimen design.

For polarization investigation, in addition to the alloy mentioned above, commercially pure Al and Zn wires (approximately 99.999%) were tested at different NaOH concentrations, namely 1 M, 0.1 M, and 0.01 M, to evaluate the alloy at pH 14, 13, and 12, respectively. The wire diameters of Al and Zn wires were 0.15 and 0.2 cm, respectively. Once the specimens were cut, they were cleaned using water and acetone, and a connecting cable was soldered on the surface close to one of the ends of the specimens to allow for an electrical connection. Soldering was carried out by using soldering iron and tin/lead solder. The iron was heated to a high temperature to melt the solder to join the cable. Furthermore, at the interface, a region of approximately 2.5 cm was coated with epoxy to prevent the formation of crevices. The specimens were then mounted with epoxy resin using a metallography sample holder to allow for stability. Figure 3 shows a schematic illustration of the electrode design. Before testing, all samples were kept at the open circuit potential for some time around twenty minutes to allow for potential stabilization. Potentiodynamic polarization tests were carried out by scanning the potential from −0.1 V below the open-circuit potential (cathodic curve), up to 1.1 V above the open-circuit potential (anodic curve), at a rate of 0.1 mV/s. Anodic polarization can be used to study the passive behavior of a given metal–electrolyte system [21].

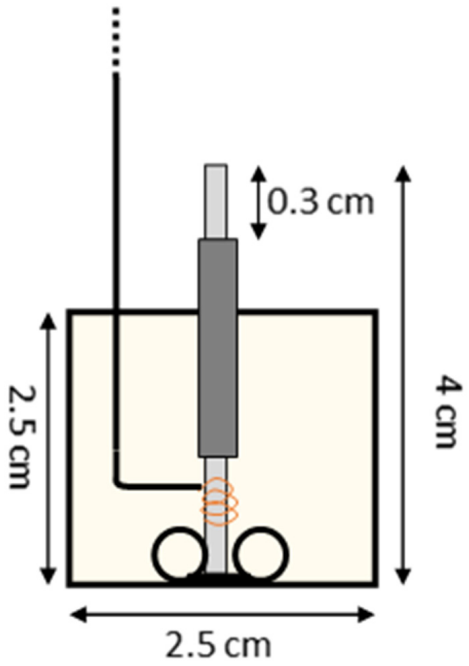

Figure 3. Front-side view of the electrode that was designed for potentiodynamic polarization testing.

2.2. Designing of a Titanium Reference Electrode

Because of the high pH of the solution used during the exposure of the specimens, the use of a conventional electrode such as a saturated calomel electrode (SCE) is not recommended. This is because continuous exposure to the solution can degrade the membrane of the electrode and damage it beyond repair. Therefore, an alternative to the traditional approach for measuring potentials is necessary. The use of activated titanium rod (ATiR) electrodes has been described by Castro et al. [22], whereby a titanium rod coated with oxides of precious metals (typically ruthenium oxide) has been successfully used as an alternative for reference electrodes (REs). The advantage of this type of RE lies in its inertness since it does not interfere with the chemistry of the solution, just as the solution does not interfere with the chemistry of the coating of the ATiR [23]. Titanium cannot be spot-welded or soldered; therefore, this electrode was manufactured by performing the steps shown in Figure 4.

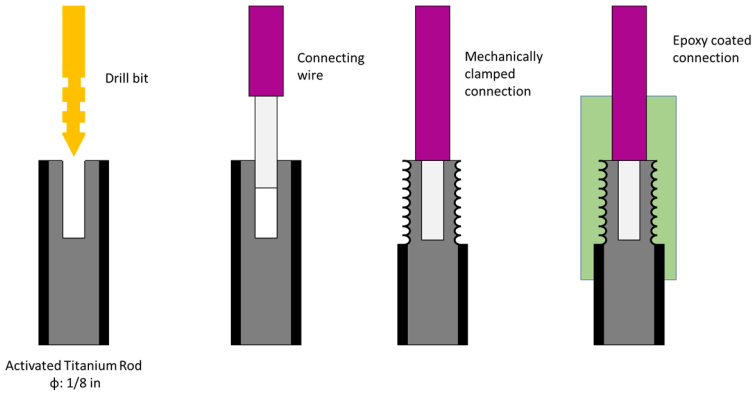

Figure 4. Series of steps for manufacturing ATiR reference electrode.

2.3. Experimental Cell Design

The testing cell, shown in Figure 5, consisted of a cylindrical section of plexiglass held together using metallic rods attached to the base and the cover. Seven specimens were simultaneously tested in each test run. Potentials were recorded every 60 s by means of an Orion data logger using the TracerDAQ software provided by the manufacturer. The prepared ATiR was used as a reference electrode. An activated titanium mesh was also part of the cell as a counter electrode for electrochemical measurements.

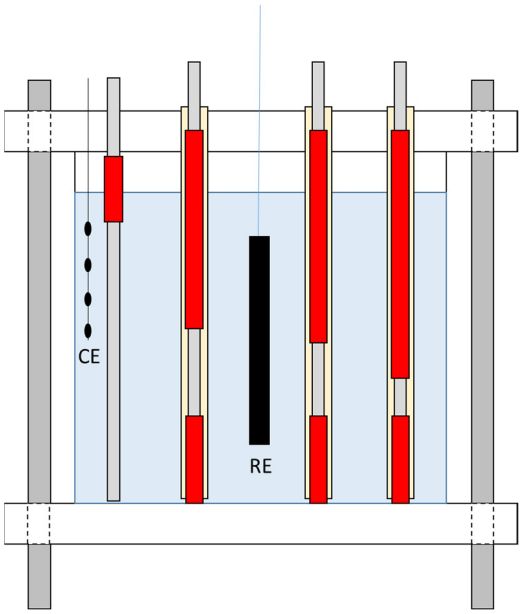

Figure 5. Schematic illustration of the testing cell setup.

Additionally, in this cell, electrochemical impedance spectroscopy (EIS) was conducted with a frequency sweep from 100 kHz to 10 mHz to assess the corrosion rates of the specimens when active and when they transitioned into a passive state using a GAMRY potentiostat. Using this method, the value for the polarization resistance R_p was obtained.

3. Results

The potentiodynamic polarization results, with a scan rate of 0.1 mV/s, are shown in Figures 6 and 7, for commercially pure Zn and Al, respectively. The polarization behavior was determined in NaOH solutions, at pH = 12, 13, and 14. Figure 8 shows a comparison of the potentiodynamic polarization for three different types of electrodes: bare without a crevice, with crevice, and completely lacquered. Superimposed on the figure is the marking of the active–passive transition boundary potential (E_{pass}) [2].

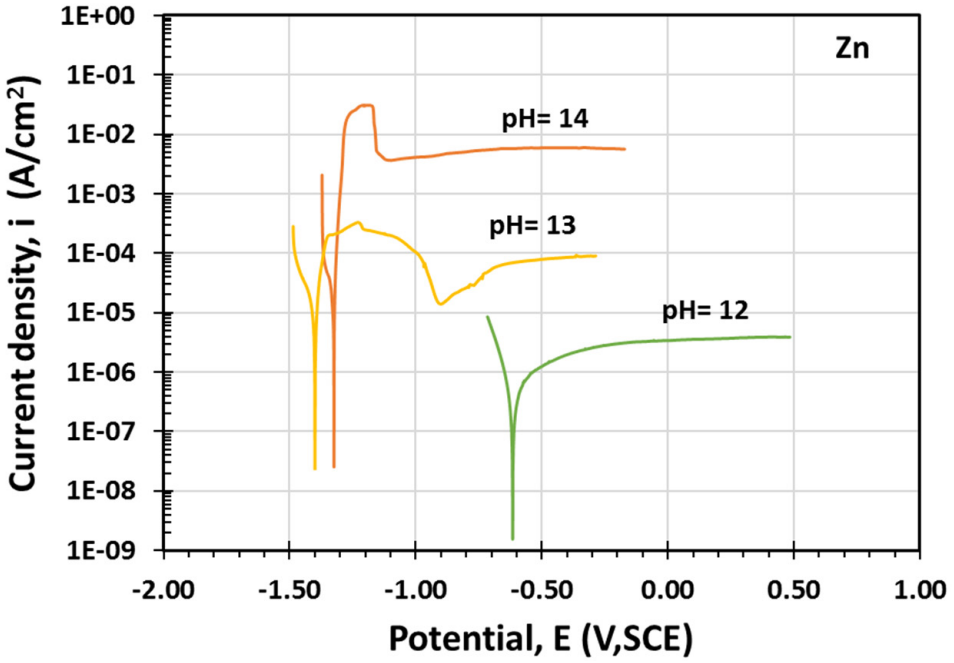

Figure 6. Polarization curves of commercial pure Zn exposed to NaOH solutions at pH = 12, 13, and 14. The sweep rate was 0.1 mV/s.

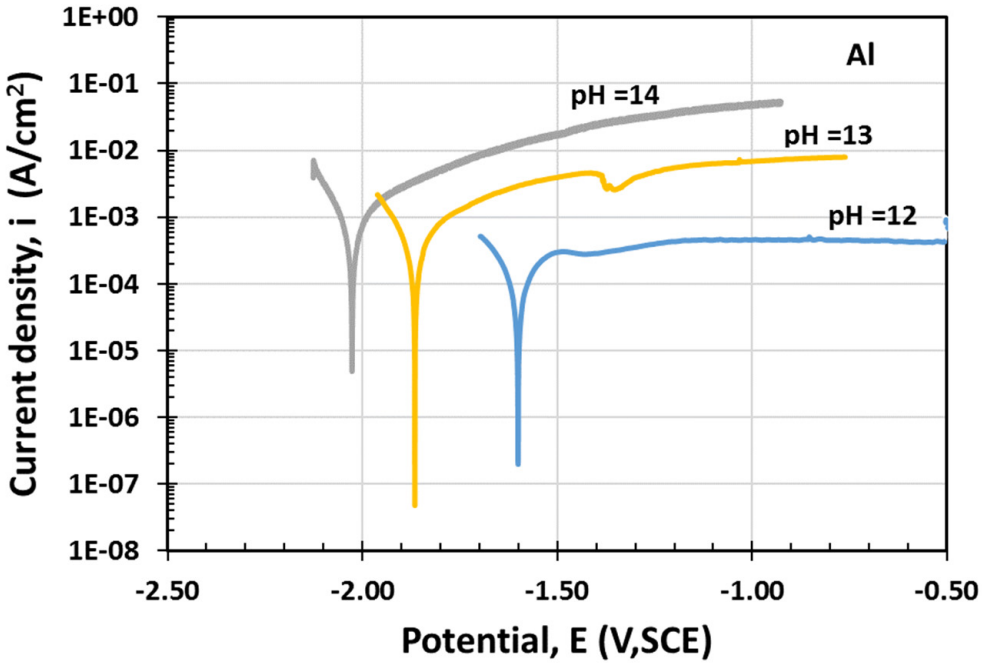

Figure 7. Polarization curves of commercial pure Al exposed to NaOH solutions at pH = 12, 13, and 14. The sweep rate was 0.1 mV/s.

The transient open-circuit potential behaviors for the Zn-2%Al crevice electrodes exposed to 1M NaOH are shown in Figures 9 and 10, at room temperature. Figure 9 illustrates the results for electrodes with dimensions of X = 30 mm and Y = 30, 15, and 7 mm. Figure 10 demonstrates the results for electrodes with the same Y dimensions but with X = 7 mm. Occasionally, bubbles were found to generate from the electrode at different times. For accuracy purposes, duplicate electrodes were used.

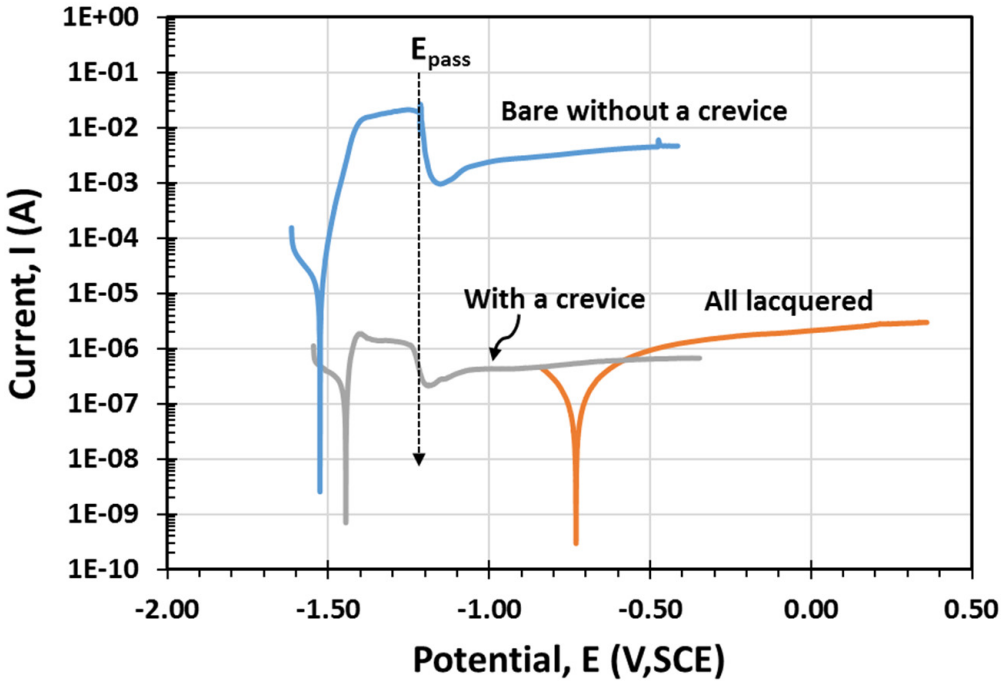

Figure 8. Polarization curves of Zn-2%Al electrodes exposed to 1M NaOH solutions. Three different types of electrodes were tested: bare without a crevice, with a crevice, and completely lacquered. The sweep rate was 0.1 mV/s at room temperature.

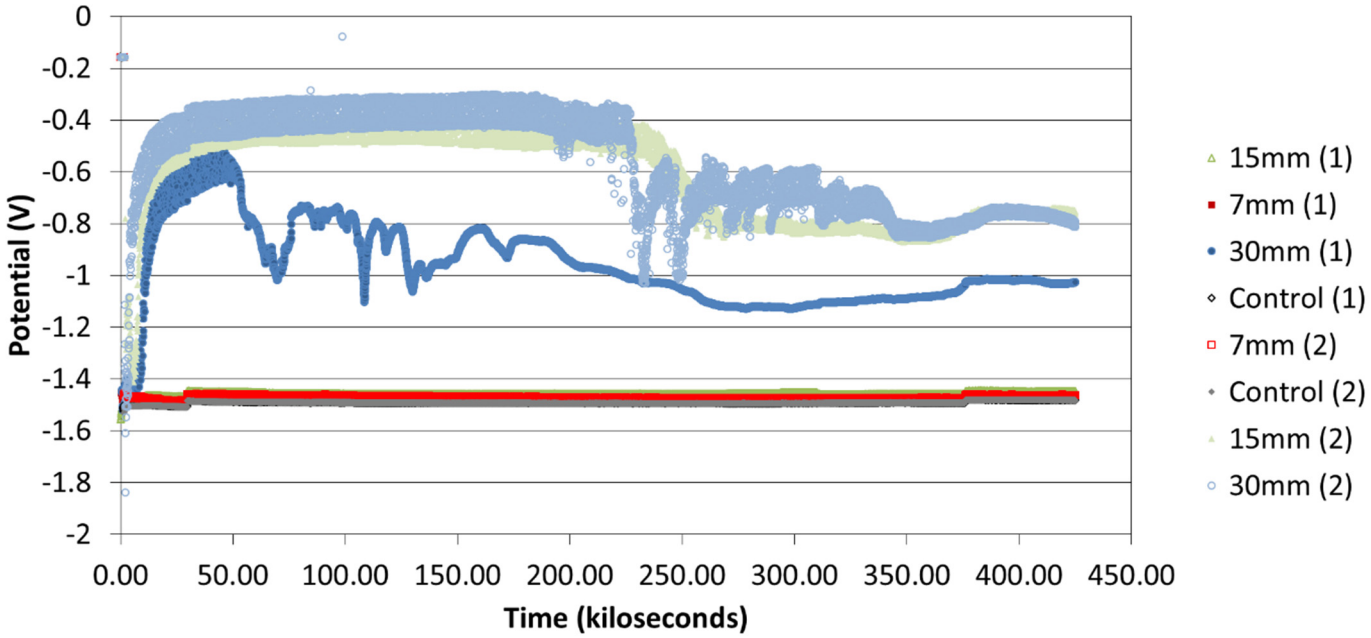

Figure 9. Potential (vs. SCE) transient behavior of electrodes with X = 30 mm and Y = 30, 15, and 7 mm, showing a jump in potential to more noble values.

Another setup was established to test crevice corrosion, for a situation that resembled exposing the disbonded region of the polymer coating on Zn-2%Al used for rebar protection to ambient air instead of concrete pore solution surrounding all sides. For this purpose, the same Zn-2%Al alloy and the plastic tubing were used to generate a crevice. The setup was such that the crevice mouth was exposed to ambient air, while inside the crevice was exposed to the same bulk solution as used before. The duration of the experiment lasted one month. After one month, and after dissembling the crevice, severe corrosion damage was evident. The damage before and after disassembly is shown in Figure 11.

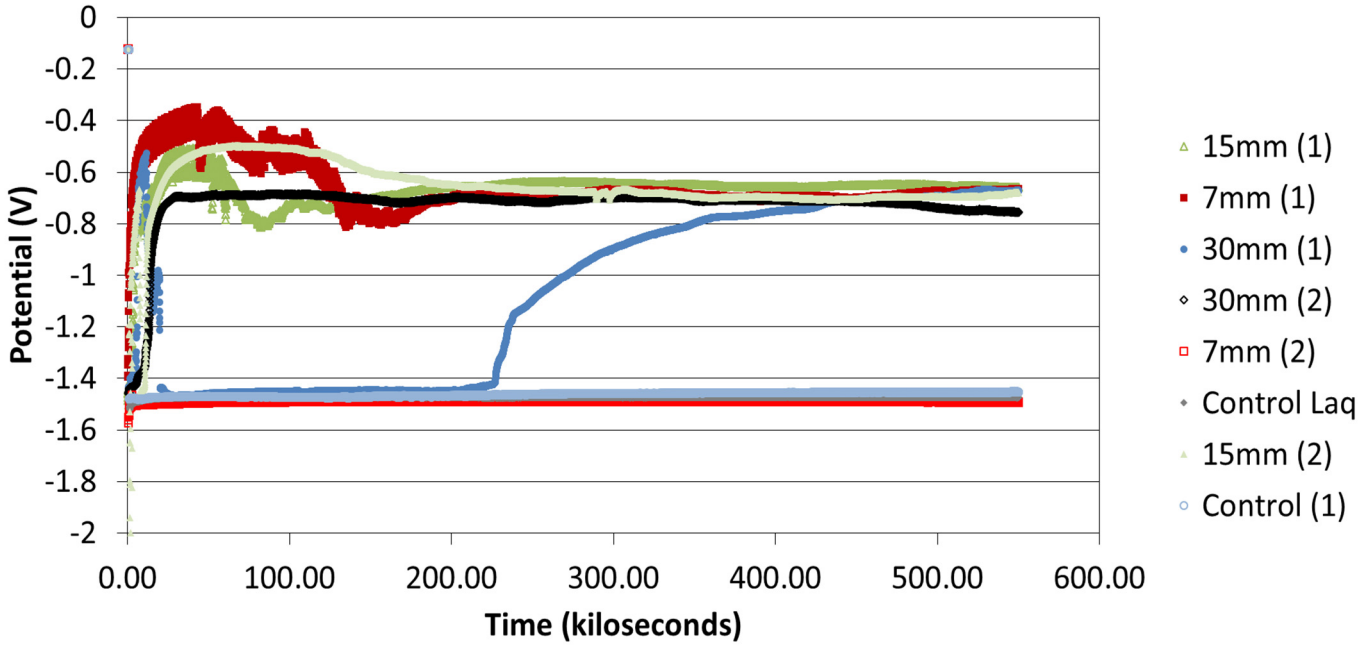

Figure 10. Potential (vs. SCE) transient behavior of electrodes with X = 7 mm and Y = 30, 15, and 7 mm, showing a jump in potential to more noble values.

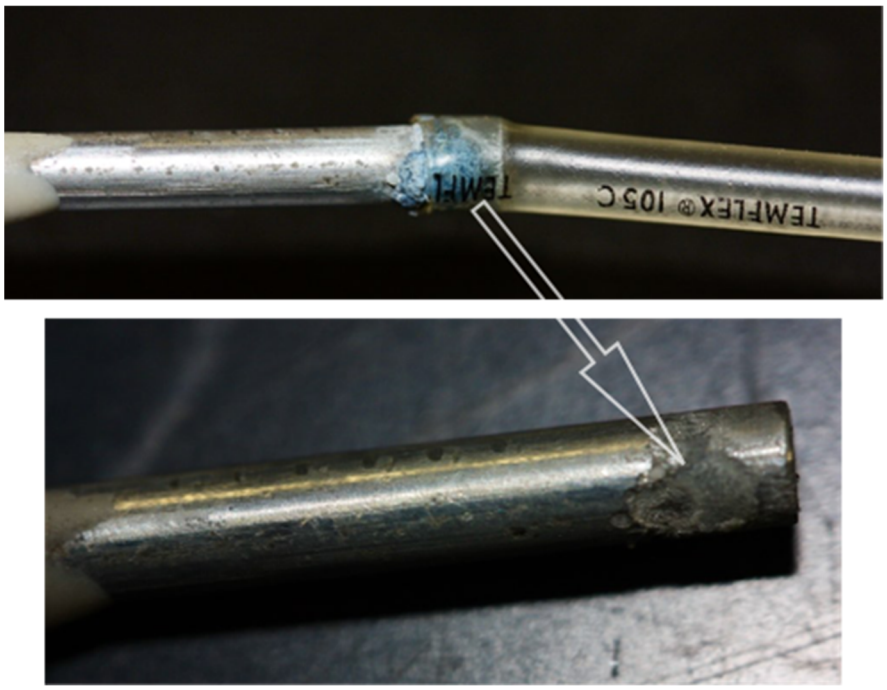

Figure 11. A photograph of the crevice parts (after the experiment) showing the surface of the zinc alloy that incurred damage. Magnification: top photo: 5×, bottom: 12×.

Figure 12 shows a Pourbaix diagram for zinc in water at 25 °C and 1 atm, generated by using a recent stability phase diagram calculation software utilizing the latest thermodynamic data [24]. The pH was adjusted by using an acid titrant, H_2SO_4, and a base titrant, NaOH. The "a" line represents the O_2/H_2O equilibrium reaction, and the "b" line represents the H^+/H_2 equilibrium reaction.

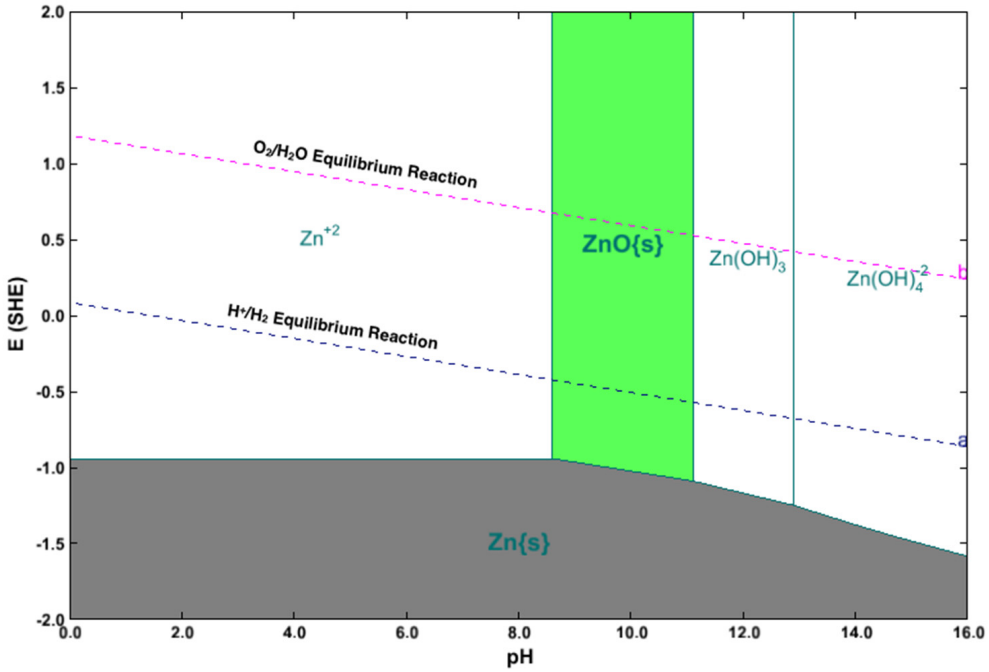

Figure 12. Pourbaix diagram for zinc in water at 25 °C and 1 atm, generated by using OLI studio software utilizing the latest thermodynamic data. The "a" line represents the O_2/H_2O equilibrium reaction, and the "b" line indicates the H^+/H_2 equilibrium reaction.

The EIS spectrum of the Zn-2%Al alloy specimen with a crevice is shown in Figure 13. For the control specimens, the spectra are shown in Figures 14 and 15, which exhibit a slight difference in behavior, showing different shapes for the semicircle. One semicircle is also seen for spectra generated at pH 12, 13, and 14 when conducting EIS on Zn-2%Al specimens used for polarization testing at the initial time after stabilizing the open-circuit potential and before starting the polarization. R_p was nearly 500 Ω when the material was exposed to a solution with pH 14 and 13, while it jumped to 50,000 Ω when exposed to pH 12. Additionally, the solution resistance (R_s) increased by a factor of 10 each time the pH changed, dwindling down from approximately 2.5 Ω at pH 14, to 20 Ω at pH 13, and nearly 175 Ω at pH 12. This agrees with the solution becoming diluted by a factor of 10 each time the pH changed by one unit: 12, to 13, to 14.

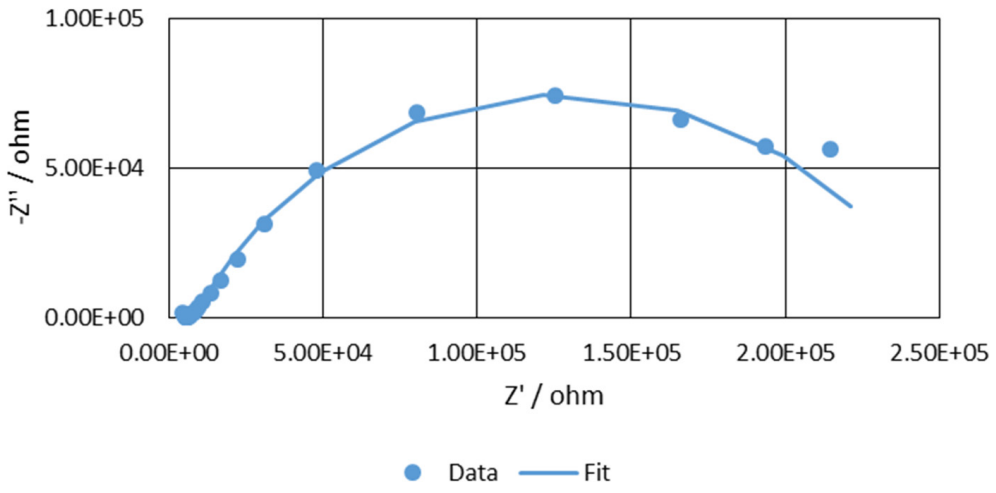

Figure 13. Typical EIS spectrum of Zn-2%Al specimens with crevice.

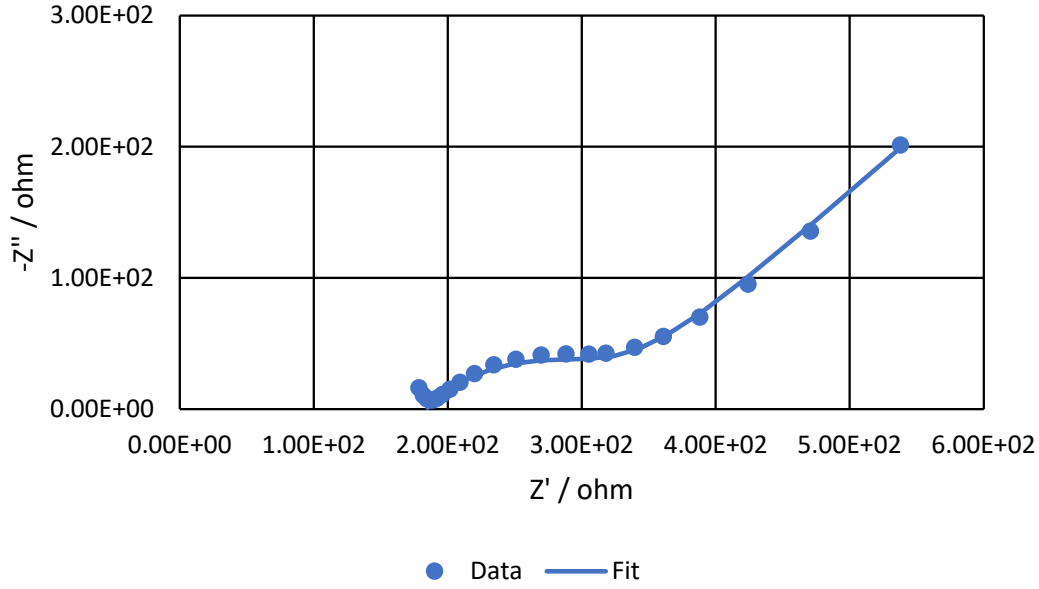

Figure 14. Typical EIS spectrum of specimens coated with lacquer.

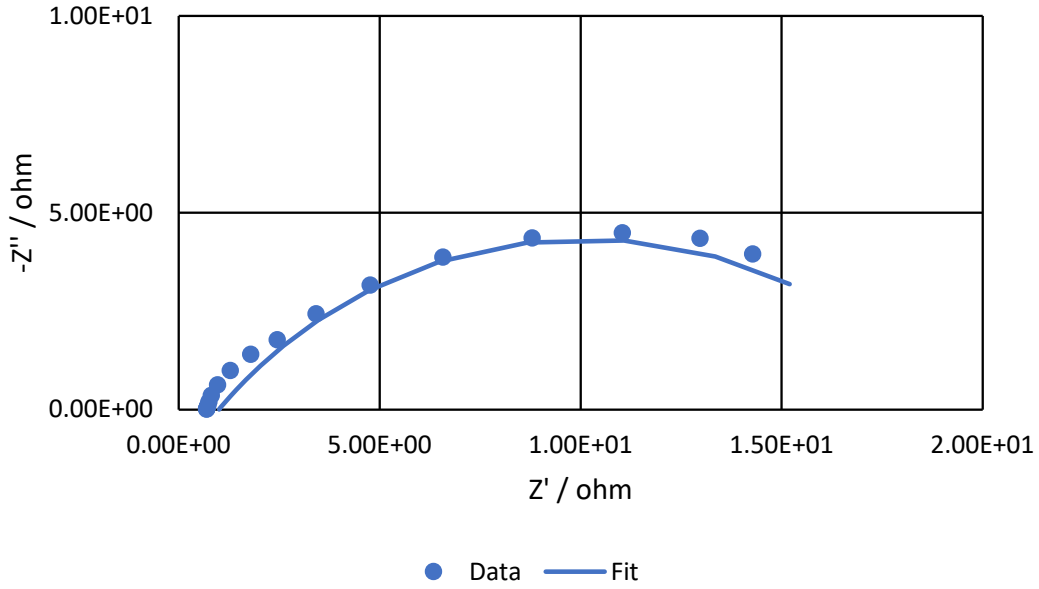

Figure 15. Typical EIS spectrum of uncoated specimens.

When testing aluminum samples in all pH solutions, the typical EIS response was that of two semicircles, as shown in Figure 16. For R_p, the value tripled to approximately (75 Ω) when the pH dropped from 14 to 12. However, in the case of Zn (Figure 17), a well-defined semicircle was observed. R_p values were low for specimens exposed to pH 14 and 13 (200 Ω and 300 Ω, respectively), whereas for pH 12, they averaged approximately 90,000 Ω.

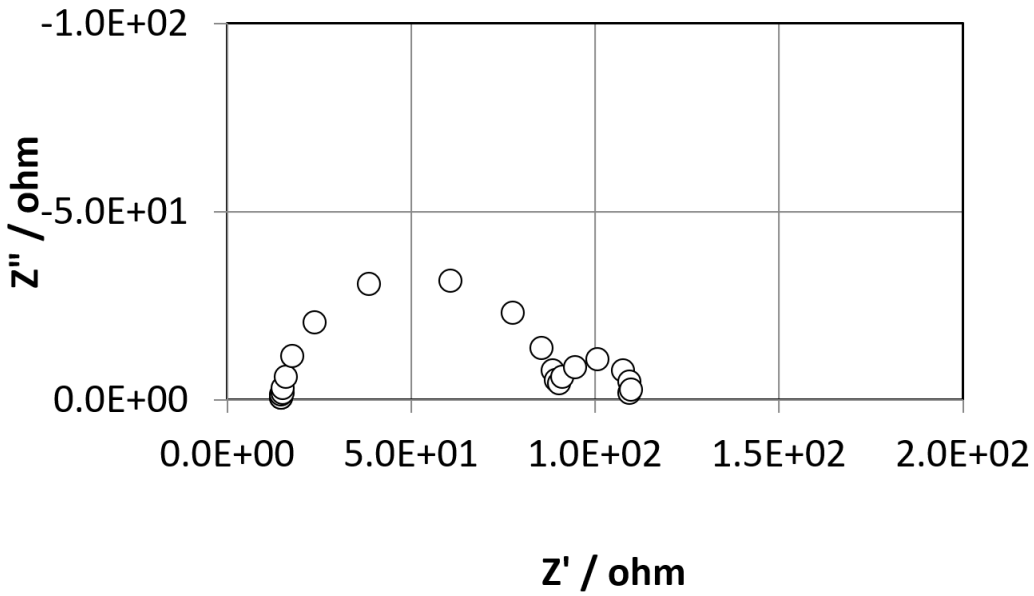

Figure 16. Typical EIS spectrum obtained for aluminum samples.

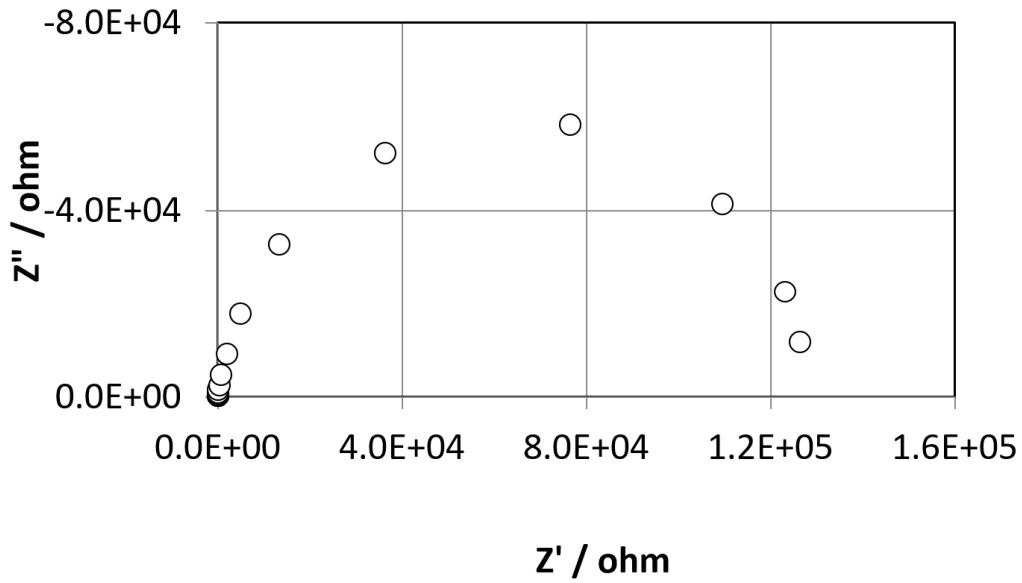

Figure 17. Typical EIS spectrum observed for bare Zn samples showing passivation.

4. Discussion

The potentiodynamic polarization results for the Zn (Figure 6) showed a clear trans/passive behavior at higher pH values of 13 and 14. The transition boundary potential (E_{pass}) shifted to higher potentials when the pH decreased. The passivation currents were relatively high and were reduced by almost two orders of magnitude when the pH decreased from 14 to 13. A high passivation current suggests the occurrence of possibly slowly dissolving oxides and the formation of a corrosion film that does not protect the entire surface. On the other hand, the polarization results for Al (Figure 7) revealed an active condition for all the pH values tested. Even for the case at pH 12, the passive current was two orders of magnitude higher than the counterpart of Zn. Interestingly, polarization testing on Zn-5%Al alloy showed a behavior similar to that of Zn reported here [25]. Therefore, we can conclude that, for the Zn-2%Al, Zn controls the electrochemical behavior of the overall alloy. This is also supported by the nature of the microstructure of this alloy, which consists of separate phases and lacks any intermetallic compounds [25].

For Zn-2%Al electrodes with crevices exposed to the 1 M NaOH solution without any polarization, the transient potentials shown in Figures 9 and 10 reveal a jump of approximately 0.9 V from −1.5 V vs. SCE to −0.6 V vs. SCE. A similar trend was seen when X = 15 mm. The potential jumps instead of drops support the hypothesis of passivation occurring inside the crevice portion of the specimen. It is speculated that, initially, crevice corrosion occurs inside the crevice which leads to the formation of Zn complexes with hydroxide ions, shifting the water dissociation reaction to hydrogen production and thereby lowering the pH. Therefore, this could lead to a condition inside the crevice where both the pH and the oxygen content are lower than in the bulk of the solution [26]. The decrease in pH may allow Zn-Al alloy to shift toward a passive regime by forming stable and more protective oxides, thus shifting the potential toward more noble values [27]. A passive ZnO layer was suggested to form in a KOH solution [28]. This scenario is also expected according to the Pourbaix diagram shown in Figure 12. Interestingly, from the current experimental results, the potential jump −0.6 V vs. SCE matches more with the corrosion potential at pH = 12, showing a passive surface, as seen in Figure 6. Additionally, the control bare specimens showed no jump in potential throughout the experiments. This further indicates that there is a change in the local chemistry inside the crevice that leads to the passivation of the specimens whenever a crevice is present.

4.1. Effect of Ambient Air

The condition shown in Figure 11 reflects the scenario where the disbonded region of the polymer coating on Zn-2%Al used for rebar protection was partially exposed to ambient air instead of the concrete pore solution. The figure shows that severe crevice corrosion occurred. A possible interpretation of this finding is that carbonation close to the surface occurred. Atmospheric carbon dioxide (CO_2) possibly reacted chemically with the water and formed carbonic acid. Evidently, zinc will corrode when the pH goes below 8.6. Therefore, the carbonation process leads to acidification, promoting the corrosion of Zn inside the crevice. A similar interpretation was reported elsewhere [9].

4.2. EIS Investigation

To analyze the typical impedance spectra seen in the results, two types of equivalent circuits were used. One setup consisted of a circuit when the EIS spectra contained two semicircles, and then a modified equivalent circuit was used to evaluate the coatings (Figure 18). By contrast, for the second type, the EIS spectra exhibited one semicircle, and then a modified Randles circuit was used (Figure 19). Once R_p values were obtained and multiplied by the area, using the Stern–Geary equation, the corrosion current density was obtained [29] as follows:

$$i_{corr} = B/R_p \quad (1)$$

where [30]:

$$B = \frac{\beta_a \bullet \beta_c}{\beta_a + \beta_c};\ \text{for zinc}\ B \sim 0.022\text{V} \quad (2)$$

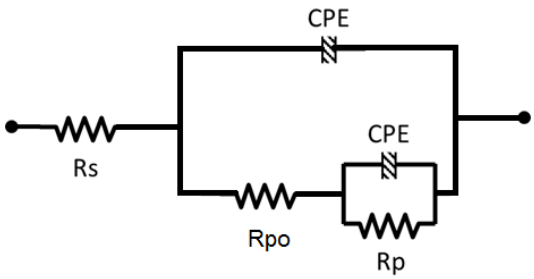

Figure 18. The modified Randles circuit used to fit EIS data.

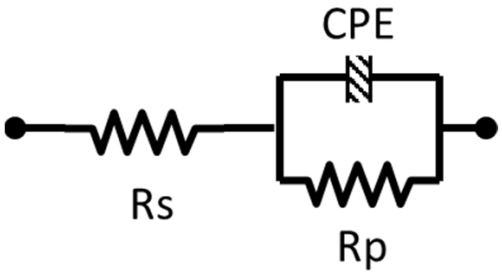

Figure 19. The modified Randles equivalent circuit used to fit EIS data.

An estimation of the corrosion rate as penetration per unit of time was obtained using the Faradaic conversion for zinc, where 1 μA/cm^2 corresponds to approximately 15 μm/y.

The trend of the EIS data collected for Zn-2%Al alloy showed high values of impedance for specimens with crevices (Figure 13), which could be attributed to the relatively small area exposed, whereas controls (Figures 14 and 15) showed very little resistance. In general, control experiments showed an average apparent corrosion rate of ~0.75–3 μm/y. When analyzing the EIS data of the specimens subjected to crevices, with high values of impedance, the corrosion rates of the specimens were higher than the controls. This is likely due to the small surface area that was assumed in the analysis to be exposed. However, it is important to point out that even though the controls were coated with lacquer, they still showed to be in an active regime. This is likely a result of imperfections in the coating, on a microscale, that may still allow for interactions between the metal and the environment. Another possibility is that a surge pass could be operating inside the small tube put on the top of the specimen, between the coated and uncoated part of the specimen, to protect against the surface effect. Accordingly, assuming the overall crevice is not just the uncoated area but rather the whole specimen, interactions are still very likely to occur between the metal in the coated sections of the specimens and the surrounding solution. Then, the overall corrosion rate agrees with the results obtained from the potential measurements.

For Zn-2%Al alloy bare specimens used for polarization testing, the EIS testing at pH 12, 13, and 14 showed a polarization resistance (R_p) value increased by about a factor of 100 when the pH was reduced to pH = 12. This again confirms that some level of passivation must have occurred during the experiment for the latter. This finding confirms the potentiodynamic polarization results of Figure 6. Zn generally passivates in a pH range of 8.6–12.5. However, for the bare Al samples and all pH values tested, a typical EIS response of two semicircles was observed, indicating the possible formation of nonprotective oxides on the surface of the specimens (corresponding to the first semicircle), as under these conditions, aluminum tends to corrode rapidly without the formation of any passive layer. This confirms our polarization results and interpretations for Al. In the case of the bare pure Zn samples that showed a well-defined semicircle, R_p values were generally low, and for specimens exposed at pH 14 and 13, R_p was in the same range and then jumped by a factor of 300 when pH was decreased down to 12. This jump in R_p at pH = 12 is indicative of the occurrence of passivation at pH = 12, similar behavior to that seen for Zn-2%Al alloy.

In summary, EIS results suggest that the passivation properties of the Zn-2%Al alloy are granted by the presence of Zn in the alloy. Once the R_p was normalized with the area and transformed to current densities by means of the Faradaic conversion, aluminum showed higher current densities throughout all levels of pH tested (Figure 20), ranging from almost 2000 μA/cm^2 to about 500 μA/cm^2. Zn only showed a fraction of the aluminum current density in all cases, which is not surprising as the Pourbaix diagram for aluminum suggests a passive regime in the pH range of ~4–8.5 [15].

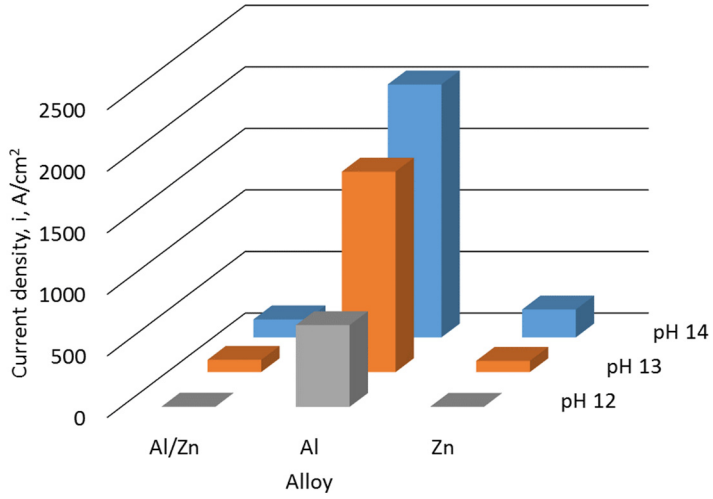

Figure 20. Average current densities determined with EIS for each alloy.

The results of a comparison of the current density of Zn-2%Al specimens under different conditions (with crevice, fully lacquered with no crevice, and partially lacquered leaving only "Y" areas not lacquered) are shown in Figure 21. It can be seen that lacquer is pivotal in the protection of the area of the specimen that needs to be protected from the solution. Any current identified may be the effect of local resistance provided by the lacquer and the medium, or the other possibilities discussed before. In the presence of a crevice, however, the current density is relatively small, which may be an effect of a decrease in the local pH in the crevice due to the depletion of OH^- ions. In the absence of one, however, the current density increased by about three orders of magnitude, indicative of an active condition due to the interaction of the metal with an alkaline-rich environment. A similar behavior was observed when potentiodynamic scans were conducted for these three conditions of specimen setups, as shown in Figure 8. Interestingly, for the fully lacquered specimen with no crevice setup, the corrosion potential and the entire polarization curve agree with the polarization curve of pure Zn at pH 12, shown in Figure 6. This corrosion potential is near the maximum value measured of the potential transient (Figures 9 and 10), showing a passive condition. A possible explanation of this finding is that the imperfections on the lacquer could have made microcrevices that enhanced stagnation and therefore led to the formation of stable passive oxides, along with a reduction in pH.

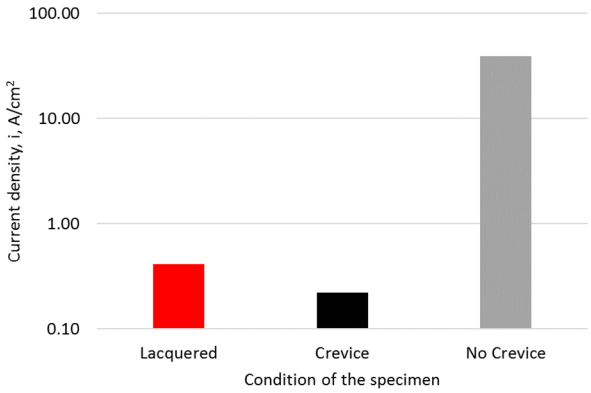

Figure 21. The current density of specimens as a function of their condition in the system.

5. Conclusions

- Potential transient of Zn-2%Al specimens with crevice showed signs of passivation occurring after a few hours of exposure, at which the open-circuit potential shifted toward much more noble values.

- The elemental Al dissolution rate did not have a significant effect on the mechanism of Zn-2%Al dissolution or passivation. This is based on the EIS testing on Zn, Zn/Al, and Al alloys, indicating that passivation is associated more with Zn than with Al.
- The EIS results show high impedance values of the specimens with crevices; however, this can be attributed to the relatively small area of exposure. Apparent corrosion rates showed that all active specimens corroded at relatively the same rate (~0.75–3 µm/y).

The current analysis suggests that if the disbonding of the polymer coating occurs with dual-protected concrete rebar, passivation is more likely to occur, which protects the outer surface of the galvanization layer from the side with the polymer coating.

Funding: This research received no external funding.

Data Availability Statement: Not applicable.

Acknowledgments: E. Paz-Velásquez, Department of Civil and Environmental Engineering, University of South Florida, Tampa, FL, USA, helped with running experiments and generating EIS data.

Conflicts of Interest: The author declares no conflict of interest.

References

1. Abdulsalam, M.I. Behaviour of crevice corrosion in iron. *Corros. Sci.* **2005**, *47*, 1336–1351. [CrossRef]
2. Ding, J.; He, W.; Liu, Y.; Zhang, C.; Wang, H.; Han, E.-H. Numerical Simulation of Crevice Corrosion of Stainless Steel–Titanium in NaCl Solution. *Coatings* **2022**, *12*, 592. [CrossRef]
3. Fontana, M.G.; Greene, N.D. *Corrosion Engineering*; McGraw-Hill: New York, NY, USA, 1978.
4. Abdulsalam, M.I.; Presuel-Moreno, F. Investigation of crevice corrosion of metallic fastened joints in carbon fiber reinforced polymer (CFRP) exposed to coastal seawater. *Anti-Corros. Methods Mater.* **2021**, *68*, 238–247. [CrossRef]
5. Huang, X.; Zhou, K.; Ye, Q.; Wang, Z.; Qiao, L.; Su, Y.; Yan, Y. Crevice corrosion behaviors of CoCrMo alloy and stainless steel 316L artificial joint materials in physiological saline. *Corros. Sci.* **2022**, *197*, 110075. [CrossRef]
6. Xi, Y.; Wang, Q.; Wu, Y.; Zhang, X.; Dong, L.; Bai, S.; Yang, Y. Crevice corrosion behavior and mechanism of laser additive manufacturing nickel-based alloy under wedge-shaped crevice by using wire beam electrode. *Anti-Corros. Methods Mater.* 2023, *ahead-of-print*. [CrossRef]
7. Huang, S.; Wu, W.; Su, Y.; Qiao, L.; Yan, Y. Insight into the corrosion behaviour and degradation mechanism of pure zinc in simulated body fluid. *Corros. Sci.* **2021**, *178*, 109071. [CrossRef]
8. Zhai, X.; Li, K.; Guan, F.; Wang, N.; Agievich, M.; Duan, J.; Hou, B. Ultrasound-assisted synthesis of wear-resistant Zn-Ferrocene composite coatings with high anticorrosive properties in alkaline environments. *Surf. Coat. Technol.* **2018**, *356*, 19–28. [CrossRef]
9. Abdulsalam, M.I. Study of simulated disbonded polymer film on Zn-Al alloy coated reinforcing steel rebars. *Corros. Sci.* **2018**, *138*, 307–318. [CrossRef]
10. Vu, T.N.; Volovitch, P.; Ogle, K. The effect of pH on the selective dissolution of Zn and Al from Zn–Al coatings on steel. *Corros. Sci.* **2013**, *67*, 42. [CrossRef]
11. Nomura, H.; Kimata, Y.; Kanai, H. Corrosion Resistance of Prepainted Zn-11%Al-3%Mg-0.2%Si Coated Steel Sheet. In Proceedings of the International Conference on Zinc and Zinc Alloy Coated Steel, Galvatech'04, Warrendale, PA, USA, 4–7 April 2004; p. 763.
12. Manna, M.; Dutta, M.; Bhagat, A.N. Microstructure and Electrochemical Performance Evaluation of Zn, Zn-5 wt.% Al and Zn-20 wt.% Al Alloy Coated Steels. *J. Mater. Eng. Perform.* **2021**, *30*, 627–637. [CrossRef]
13. Al-Negheimish, A.; Hussain, R.R.; Alhozaimy, A.; Singh, D.D.N. Corrosion performance of hot-dip galvanized zinc-aluminum coated steel rebars in comparison to the conventional pure zinc coated rebars in concrete environment. *Constr. Build. Mater.* **2021**, *274*, 121921. [CrossRef]
14. Tittarelli, F.; Mobili, A.; Giosuè, C.; Belli, A.; Bellezze, T. Corrosion behaviour of bare and galvanized steel in geopolymer and Ordinary Portland Cement based mortars with the same strength class exposed to chlorides. *Corros. Sci.* **2018**, *134*, 64–77. [CrossRef]
15. Pourbaix, M. *Atlas of Electrochemical Equilibria in Aqueous Solutions*; National Association of Corrosion Engineers: Houston, TX, USA, 1974.
16. Permeh, S.; Lau, K. Corrosion of galvanized steel in alkaline solution associated with sulfate and chloride ions. *Constr. Build. Mater.* **2023**, *392*, 131889. [CrossRef]
17. Lau, K.; Sagüés, A.A. Corrosion of epoxy- and polymer/zinc-coated rebar in simulated concrete pore solution. *Corrosion* **2009**, *65*, 681–694. [CrossRef]
18. Halder, A.K.; Manna, M.; Chakraborty, A.; Bhagat, A.N. Analysis of early failure of galvanised borewell pipe. *Eng. Fail. Anal.* **2021**, *133*, 105957. [CrossRef]
19. Zhang, W.; Liu, H.; Hu, M.; Wu, W. Microenvironment evolution and SCC behavior of subsea pipeline within disbonded coating crevice in a seawater environment under cathodic protection. *Anti-Corros. Methods Mater.* **2021**, *68*, 77–84. [CrossRef]

20. *PA 19428-2959*; Standard Specification for Zinc and Zinc Alloy Wire for Thermal Spraying (Metallizing) for the Corrosion Protection of Steel. ASTM International: West Conshohocken, PA, USA, 2013.
21. Zhang, S.; Li, Z.; Su, X.; Yang, C. Experimental Data Treatment of the Pipeline Steel Polarization Curve under AC Interference. *Int. J. Electrochem. Sci.* **2019**, *14*, 10888–10906. [CrossRef]
22. Castro, P.; Sagüés, A.A.; Moreno, E.I.; Maldonado, L.; Genescá, J. Characterization of activated titanium solid reference electrodes for corrosion testing of steel in concrete. *Corrosion* **1996**, *52*, 609. [CrossRef]
23. Sagues, A.A.; Moreno, E.I.; Morris, W.; Andrade, C. Characterization of a solid reference electrode for corrosion measurement of steel in concrete. In *Proceedings of the First Mexican Symposium on Metallic Corrosion*; Maldonado, L., Pech, M., Eds.; UNAM Facultad de Quimica Press: Mexico City, Mexico, 1995; pp. 43–52, Paper 64; ISBN 968-36-4811-8.
24. *OLI Studio Corrosion Analyzer*, Version 9.3; OLI Systems, Inc.: Cedar Knolls, NJ, USA, 2016.
25. Vu, T.; Mokaddem, M.; Volovitch, P.; Ogle, K. The anodic dissolution of zinc and zinc alloys in alkaline solution. II. Al and Zn partial dissolution from 5% Al–Zn coatings. *Electrochim. Acta* **2012**, *74*, 130–138. [CrossRef]
26. Rosenfeld, I.L.; Marshakov, I.K. Mechanism of Crevice Corrosion. *Corrosion* **1964**, *20*, 115t–125t. [CrossRef]
27. Shang, X.-L.; Zhang, B.; Han, E.-H.; Ke, W. Effect of small addition of Mn on the passivation of Zn in 0.1M NaOH solution. *Electrochim. Acta* **2011**, *56*, 1417–1425. [CrossRef]
28. Yuan, Y.; Zhou, Z.; Luo, J.; Dan, Z.; Qin, F.; Chang, H. (1 1 1)-facet dominant ultrafine nanoporous silver as SERS substrates with high sensitivities and ultrahigh detection limits. *Appl. Surf. Sci.* **2021**, *556*, 149820. [CrossRef]
29. Stern, M.; Geary, A.L. Electrochemical polarization I. A theoretical analysis of the shape of polarization curves. *J. Electrochem. Soc.* **1957**, *104*, 56–63. [CrossRef]
30. Jones, D.A. *Principles and Prevention of Corrosion*, 2nd ed.; Prentice Hall: Hoboken, NJ, USA, 1995.